A Novel Graph-Based Characterization of Peritumoral Vascular Architecture for Pre-Treatment Assessment of Radiation Necrosis Risk in Brain Metastases

Yi Lao[1], Tyler Watkins[1], Terence Williams[1], Stephanie Yoon[1], Wensha Yang[2], Ke Sheng[2], An Liu[1]
[1]Radiation Oncology, City of Hope National Medical Center [2] Radiation Oncology, University of California, San Francisco

2026 JULY 19–22 VANCOUVER, BC
JOINT AAPM | COMP MEETING

ABSTRACT

Pre-treatment heterogeneity in vascular architecture may contribute to differential susceptibility to radiation necrosis (RN), a dose-limiting toxicity of stereotactic radiosurgery (SRS). Using routine pre-treatment MRI from 76 brain metastases, including 24 with RN, we developed a novel graph-based framework (VasGraph) to quantitatively characterize peritumoral vascular topology and evaluate RN risk. RN-prone tumors exhibited reduced vascular network capacity and efficiency, and multivariate integration of VasGraph metrics further improved RN prediction. These findings provide evidence that pre-treatment peritumoral vascular architecture is involved in subsequent RN development. The proposed VasGraph framework, for the first time, noninvasively leverages this information to improve RN prediction, supporting pre-treatment risk stratification and personalized treatment planning.

CONTACT

Yi Lao
City of Hope National Medical Center
1500 E. Duarte Road, Duarte, CA 91010
yilao@coh.org

INTRODUCTION

Radiation necrosis (RN) is a dose-limiting toxicity of stereotactic radiosurgery (SRS) for brain metastases [1-2].

Biological Rationale: Although its etiology remains inadequately understood, growing evidence implicates vascular injury and blood–brain barrier disruption as key mechanisms [3]. RN develops in only a subset of lesions exposed to similar high radiation doses, indicating that dose alone does not fully explain risk and that pre-existing vascular heterogeneity may influence susceptibility to radiation-induced injury.

The Gap: Most prior studies have focused on dose-based predictors or post-treatment imaging for diagnosis, with limited emphasis on pre-treatment vascular interrogation.

Here, we introduce a novel graph-based framework to quantitatively characterize peritumoral vascular topology from pre-treatment contrast-enhanced MRI for identifying lesions prone to RN.

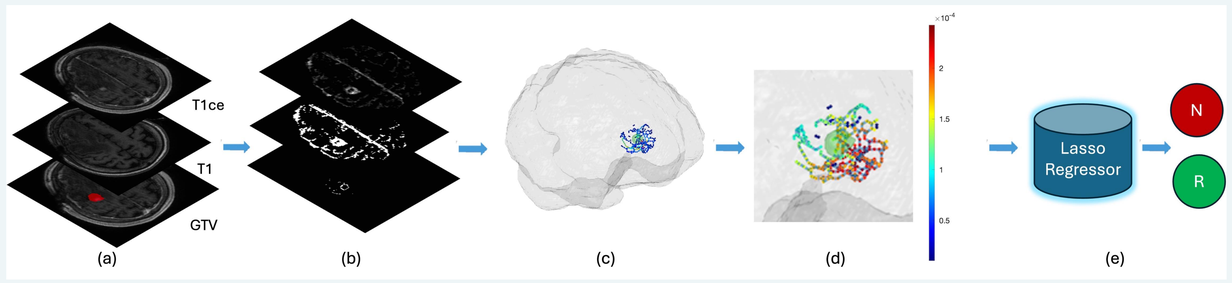

Figure 1. Illustration of the proposed pipeline for VasGraph based RN prediction. Pre-treatment T1/T1ce MRI (a) were used to extract vascular structures and generate centerline skeletons (b). VasGraph representations (c) were then constructed by tracing vascular skeletons to define nodes and edges. Graph-derived vascular topology metrics were computed (d) and subsequently integrated into a Lasso regressor to predict radiation necrosis risk (e).

METHODS AND MATERIALS

The overall pipeline for VasGraph-based RN prediction is illustrated in **Figure 1.**

Cohort: 76 brain metastases from 16 patients treated with SRS. Radiation necrosis (RN) was confirmed in 24 lesions by biopsy or ≥6-month follow-up imaging.

Vascular Extraction: Pre-treatment T1-weighted and contrast-enhanced T1 MRI were processed using subtraction-based enhancement and centerline skeletonization to extract vascular structures.

VasGraph Construction: Vascular skeletons were traced into graph-based representations, with nodes and edges defined within each tumor neighborhood (GTV + 1-cm peritumoral expansion). GTV-restricted subgraphs were also analyzed.

Statistical Analysis: Seven categories of graph-derived metrics (**Table. 1**) were computed to characterize vascular network capacity and efficiency. Individual features were assessed using univariate group comparisons and logistic regression. Multivariate Lasso regression was then used for feature selection and RN risk prediction.

RESULTS

As intuitively illustrated in **Figure 2**, RN-prone tumors exhibit visibly lower node density and more fragmented vascular connections within the tumor neighborhood compared with RN-absent tumors.

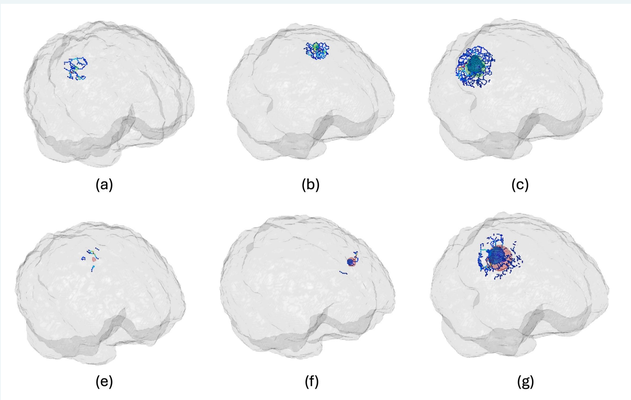

Figure 2. Illustration of VasGraph representations for three RN-absent tumors (upper row, a-c, tumor rendered in green) and three RN-prone tumors (bottom row, e-g tumor rendered in red). RN-prone tumors exhibit visibly lower node density and more fragmented vascular connections within the tumor neighborhood.

As shown in **Figures 2–3 and Table 1.** RN-prone tumors exhibited significantly reduced betweenness in the tumor neighborhood (BEC, AUC = 0.76, p = 0.001), along with reduced global efficiency (GE, AUC = 0.85, p < 0.001) and increased characteristic path length (CPL, AUC = 0.81, p = 0.001) within GTV subgraphs, indicating reduced network capacity and disrupted vascular topology.

Furthermore, under five-fold cross-validation, multivariate Lasso regression integrating VasGraph metrics achieved an AUC of 0.89 for RN prediction.

Table 1. Radiation necrosis (RN) prediction performance of VasGraph-derived metrics, including global efficiency (GE), closeness centrality (CC), edge-weighted betweenness (BEC), largest connected component (LCC), characteristic path length (CPL), node density (ND), and vascular density (VD), evaluated within the gross tumor volume (GTV) and the expanded region (GTVexp). Prediction performance from multivariate Lasso regression is also reported; four features were selected: GE (GTV), CPL (GTV), BEC (GTVexp), and ND (GTVexp), with corresponding feature distributions shown in Figure 3. .

	AUC (GTV)	p (GTV)	AUC (GTVexp)	p (GTVexp)
GE	0.85	< 0.001*	0.53	0.703
CC	0.59	0.828	0.66	0.273
BEC	0.61	0.039*	0.76	0.001*
LCC	0.58	0.005*	0.59	0.216
CPL	0.81	0.002*	0.56	0.291
ND	0.61	0.212	0.63	0.044*
VD	0.62	0.139	0.54	0.253
	Accuracy	Sensitivity	Specificity	AUC
Lasso Regressor	0.90	0.93	0.90	0.89

RESULTS CONT.

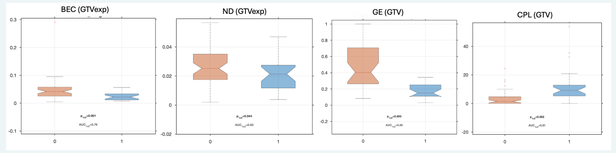

Figure 3. Box plots of the four VasGraph metrics selected by the Lasso regressor, comparing RN-prone (blue) and RN-absent (orange) tumors. RN-prone tumors exhibited significantly reduced betweenness (BEC; AUC = 0.76, p = 0.001) and node density (ND; AUC = 0.63, p = 0.044) within the tumor neighborhood, along with reduced global efficiency (GE; AUC = 0.85, p < 0.001) and increased characteristic path length (CPL; AUC = 0.81, p = 0.001) within GTV subgraphs.

DISCUSSION

1. **Explainable vascular topology differences:** As shown in Figure 2, VasGraph provides an interpretable characterization of peritumoral vascular topology, with RN-prone tumors exhibiting visibly lower node density and more fragmented vascular connections within the tumor neighborhood.

2. **Quantitative confirmation of distinct vascular architecture:** Statistical analyses (Table 1 and Figure 2) confirmed these visual observations, showing that compared with RN-absent tumors, RN-prone lesions demonstrate significantly reduced global efficiency, betweenness, and node density, along with increased characteristic path length, consistent with lower vascular network capacity in tumor neighborhoods.

3. **Predictive value for clinical risk stratification:** Integration of VasGraph metrics using multivariate Lasso regression achieved strong RN prediction performance (AUC = 0.89), highlighting the potential utility of this approach for pre-treatment risk stratification and informing treatment planning.

CONCLUSIONS

Using routine clinical MRI, we present a novel VasGraph pipeline for quantitative, interpretable characterization of peritumoral vascular topology to assess pre-treatment RN susceptibility. Graph analysis captures vascular architectural disruption associated with RN development, providing insight into vascular contributions to RN risk. These metrics enable lesion-specific vascular profiling to support pre-treatment stratification and personalized treatment planning.

REFERENCES

1. [1] Mayo, Zachary S., et al. "The dilemma of radiation necrosis from diagnosis to treatment in the management of brain metastases." Neuro-oncology 26.Supplement_1 (2024): S56-S65.
2. [2] Ahmed, Mashal, et al. "Long-Term Imaging Follow-up of Radiation Necrosis After Stereotactic Radiosurgery: A Case Report and Lessons Learned." Advances in Radiation Oncology 9.11 (2024): 101633.
3. [3] Yoritsune, Erina, et al. "Inflammation as well as angiogenesis may participate in the pathophysiology of brain radiation necrosis." Journal of radiation research 55.4 (2014): 803-811.